The Latest Development of 3D-SST
Part A: Spacetime properties of a spiral string toryx

Vladimir B. Ginzburg

Research & Development Department,
International Rolling Mill Consultants, Inc.
612 Driftwood Drive, Pittsburgh, PA 15238
www.helicola.com

Three-Dimensional Spiral String Theory (3D-SST) models the creation of hydrogen atom from quantum vacuum. Part A outlines the spacetime properties of the prime elements of nature, called toryces. Each toryx contains a circularly-propagating leading string and a toroidal trailing string propagating around the leading string at the velocity of light. Toryces are divided into four distinct topological groups based on specific combinations of inversion states of their strings. Subsequent parts of the theory show that elementary particles are formed from toryces which physical properties are directly related to their spacetime properties.

Introduction

Several models of the structure of elementary particles employ various kinds of spiral structures [1-8]. The author of this paper developed a three-dimensional spiral string theory (3D-SST) [9-18] that utilizes a toroidal spiral string element called *toryx* to model the spacetime and physical properties of the constituents of elementary particles. Toryx contains a circular leading string propagating along its circular path and a toroidal trailing string propagating around the leading string at the velocity of light in vacuum.

Toryces are divided into four distinct topological groups based on specific combinations of inversion states of their strings. Propagation of toryx leading strings obeys a derived *toryx law of motion*. Physical properties of toryces are directly related to their spacetime properties. Unification of polarized toryces produces stable elementary matter particles by following a proposed *toryx conservation law*. Toryces can exist at various excitation and oscillation quantum states, and the transitions between these states are accompanied by either absorption or radiation of the constituents of elementary radiation particles called *helyces*.

The main purpose of the Part A of the 3D-SST described in this paper is to present main features of toryces in sufficient spacetime terms, allowing one to model elementary matter particle, complex particles, such as nucleons, and, finally, the hydrogen atom. A similar approach is used in other parts of this theory to describe spacetime and physical properties of helyces that can be either subluminal or superluminal.

1 Spacetime structure and properties of the toryx

Figures A1 – A3 show the structure and main spacetime parameters of a basic toryx that does not include its fine structure. The toryx contains a circular leading string with the radius r_1 and a toroidal trailing string with the radius r_2. Leading string propagates along its circular path at the spiral velocity V_1, and trailing string propagates along its toroidal spiral path at the spiral velocity V_2. Complexity of derived spacetime parameters of the toryx is greatly affected by assumptions limiting the toryx's degrees of freedom. This paper outlines one of the simplest solutions based on the following three assumptions.

First assumption – The length of one winding of trailing string L_2 is equal to the length of one winding of leading string L_1:

$$L_2 = L_1 \qquad (-\infty < r_1 < +\infty) \tag{A1-1}$$

Second assumption – The toryx eye radius r_0 is constant:

$$r_0 = r_1 - r_2 = const. \qquad (-\infty < r_1 < +\infty) \tag{A1-2}$$

Third assumption – At each point of spiral path of trailing string its spiral velocity V_2 is constant and equal to the velocity of light c in vacuum:

$$V_2 = \sqrt{V_{2t}^2 + V_{2r}^2} = c = const. \qquad (-\infty < r_1 < +\infty) \tag{A1-3}$$

In equation (A1-3): V_{2t} = translational velocity of trailing string and V_{2r} = rotational velocity of trailing string.

Notably, although the spiral velocity of trailing string V_2 is equal to the velocity of light, equation (A1-3) prevents neither V_{2t} nor V_{2r} component of spiral velocity of trailing string from being superluminal with the other component expressed by imaginary numbers.

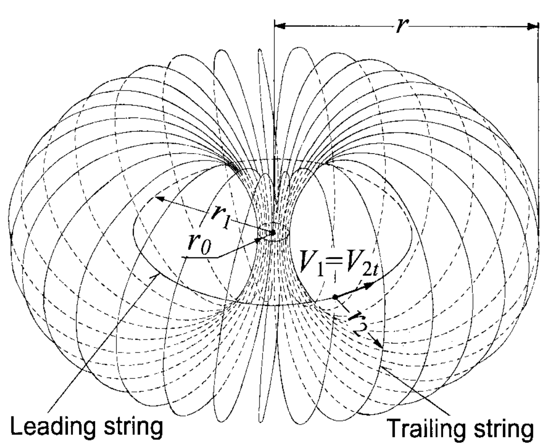

Figure A1. Isometric view of a basic toryx.

It follows from equation (A1-2) that when the radius of leading string r_1 is equal to the radius of the toryx eye r_0 the radius of trailing string r_2 reduces to zero. Consequently, the toryx transforms into a circular *real inversion toryx* with the radius r_i.

$$r_i = r_0 \tag{A1-4}$$

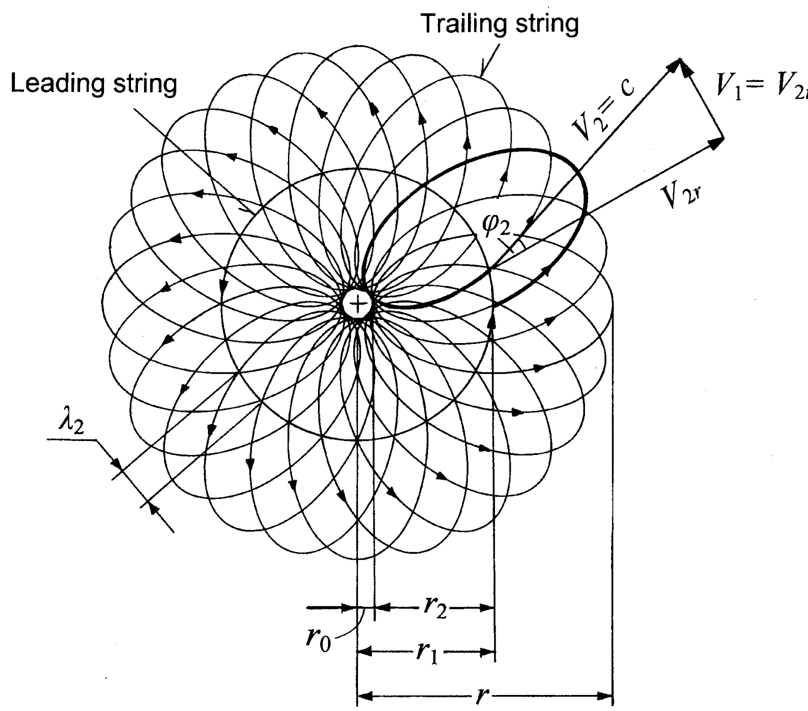

Figure A2. Top view of a toryx.

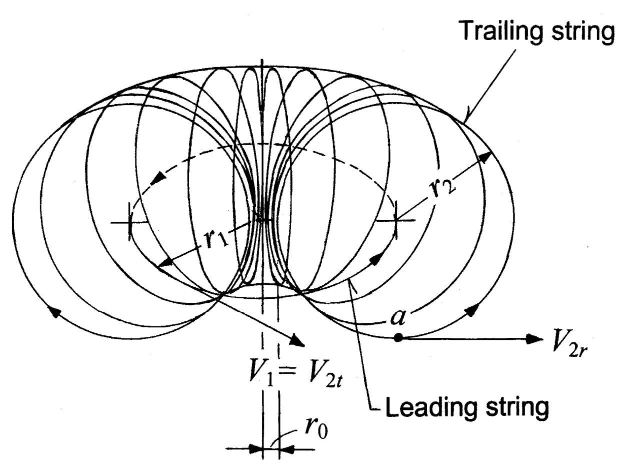

Figure A3. Cross-section of a toryx.

In the case of V_{2r} = 0 and, according to equation (A1-3), the real inversion string propagates at the constant velocity of light c with the frequency f_i equal to:

$$f_i = \frac{c}{2\pi r_i} \tag{A1-5}$$

To provide synchronous motion of trailing string with leading string, the translational velocity of trailing string V_{2t} at its point a (Fig. A3) must be equal to the spiral velocity of leading string V_1 (Fig. A4).

$$V_{2t} = V_1 \tag{A1-6}$$

Considering that the toryx parameters r_i, c and f_i are constant, we can express all toryx spacetime parameters in terms relative to these parameters. In Table A1, relative spacetime parameters of the toryx are expressed as a function of the relative radius of leading string $b_1 = r_1/r_i$.

Table A1. Toryx relative spacetime parameters as a function of the relative radius of leading string b_1 at the point a (Fig. A3).

Parameter	Leading string	Trailing string
Radius	$b_1 = \frac{r_1}{r_i}$ (A1-7)	$b_2 = \frac{r_2}{r_i} = b_1 - 1$ (A1-8)
Wavelength	$\eta_1 = \frac{\lambda_1}{2\pi r_i} = 0$ (A1-9)	$\eta_2 = \frac{\lambda_2}{2\pi r_i} = \sqrt{2b_1 - 1}$ (A1-10)
Length of one winding	$l_1 = \frac{L_1}{2\pi r_i} = b_1$ (A1-11)	$l_2 = \frac{L_2}{2\pi r_i} = b_1$ (A1-12)
The number of windings	$w_1 = 1$ (A1-13)	$w_2 = \frac{b_1}{\sqrt{2b_1 - 1}}$ (A1-14)
Translational velocity	$\beta_{1t} = \frac{V_{1t}}{c} = 0$ (A1-15)	$\beta_{2t} = \frac{V_{2t}}{c} = \frac{\sqrt{2b_1 - 1}}{b_1}$ (A1-16)
Rotational velocity	$\beta_{1r} = \frac{V_{1r}}{c} = \frac{\sqrt{2b_1 - 1}}{b_1}$ (A1-17)	$\beta_{2r} = \frac{V_{2r}}{c} = \frac{b_1 - 1}{b_1}$ (A1-18)
Spiral velocity	$\beta_1 = \frac{V_1}{c} = \frac{\sqrt{2b_1 - 1}}{b_1}$ (A1-19)	$\beta_2 = \frac{V_2}{c} = 1$ (A1-20)
Frequency	$\delta_1 = \frac{f_1}{f_i} = \frac{\sqrt{2b_1 - 1}}{b_1^2}$ (A1-21)	$\delta_2 = \frac{f_2}{f_i} = \frac{1}{b_1}$ (A1-22)
Cycle time	$\tau_4 = \frac{f_i}{f_4} = \frac{b_1^2}{\sqrt{2b_1 - 1}}$ (A1-23)	$\tau_5 = \frac{f_i}{f_5} = b_1$ (A1-24)

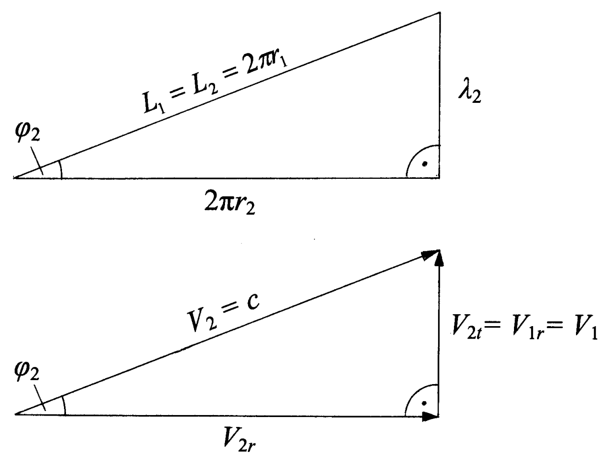

Figure A4. Spacetime parameters of the toryx strings at the middle point *a* of trailing string (Fig. A3).

The relative radius of leading string b_1 is related tot the toryx peripheral radius by the equation:

$$b_1 = \frac{b+1}{2} \qquad \text{(A1-25)}$$

The analysis of the toryx spacetime equations requires us revise several conventional mathematical terms and concepts.

2 Infinility versus a conventional zero

Conventional zero (0) is a symbol representing a complete absence of any quantity or magnitude [19,20]. As a number the zero is defined as the integer immediately preceding 1 in a conventional number line. The conventional zero is commonly used for counting of non-divisible entities, but it represents nothing that can possibly exist in nature which entities can be infinitesimally small but never reaching the absolute zero.

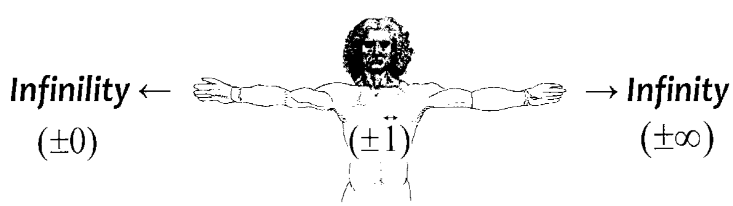

Figure A5. Infinility (± 0), infinity $(\pm\infty)$ and unity (± 1).

The 3D-SST replaces the conventional zero (0) with a new term called the *infinility* (± 0) that stands for the *infinite nil* (Fig. A5). The infinility is an inverse of infinity. One may approach the infinity by multiplying 1 by 10, 100, 1000, etc.:

$$
\begin{array}{lll}
\underline{\text{Step 1}} & 1\times 10 = 10^{1} & 1\times(-10) = -10^{1} \\
\underline{\text{Step 2}} & 1\times 100 = 10^{2} & 1\times(-100) = -10^{2} \\
\underline{\text{Step 3}} & 1\times 1000 = 10^{3} & 1\times(-1000) = -10^{3} \\
\dots & \dots & \dots \\
\text{Step}\,\infty & \to +\infty & \to -\infty
\end{array}
\qquad \text{(A2-1)}
$$

Similarly, one may approach infinility by dividing 1 by 10, 100, 1000, etc.:

$$
\begin{array}{lll}
\underline{\text{Step 1}} & 1:10 = 10^{-1} & 1:(-10) = -10^{-1} \\
\underline{\text{Step 2}} & 1:100 = 10^{-2} & 1:(-100) = -10^{-2} \\
\underline{\text{Step 3}} & 1:1000 = 10^{-3} & 1:(-1000) = -10^{-3} \\
\dots & \dots & \dots \\
\text{Step}\,\infty & \to +0 & \to -0
\end{array}
\qquad \text{(A2-2)}
$$

Notably, it requires the same number of inversely-symmetrical steps to approach infinity and infinility. The infinility and infinity are defined in a similar way. Positive infinity $(+\infty)$ is a positive quantity that is ***larger*** than any given positive quantity. Similarly, positive infinility $(+0)$ is a positive quantity that is ***smaller*** than any given negative quantity. Thus, in application to both positive infinility $(+0)$ and the negative infinilitiy (-0) we obtain:

$$
\begin{aligned}
+0 &= \frac{1}{+\infty} \\
-0 &= \frac{1}{-\infty}
\end{aligned}
\qquad \text{(A3-3)}
$$

3 String and infipoint vs conventional line and point

According to the conventional geometry, a line has neither width nor depth but can be extended on and on forever in either direction. The term "a line" is usually applied to the straight line while the term "a curved line" is used if the line is not straight. The 3D-SST replaces both above terms with a single term called *a string*. The string is based on the proposed *Spiral principle:*

Every line is a helical spiral.

This means is that what we see as either a conventional line or curved line turns out to be, upon a closer examination, a helical spiral (Fig. A6). The string corresponds to the extreme case, when the radius of the helical spiral r approaches either positive or negative infinility (± 0).

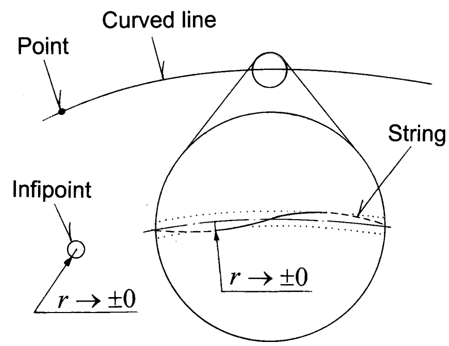

Figure A6. String and infipoint versus conventional line and point.

According to the conventional geometry, a point has neither length nor width but indicates position (Fig. A6). The 3D-SST replaces the conventional point with the proposed term *infipoint.* The infipoint is a particular case of the string which length approaches either positive or negative infinility (± 0). Consequently, the infipoint appears as a circle with the radius approaching either positive or negative infinility (± 0).

4 Toryx trigonometry vs conventional trigonometry

Conventional trigonometry is based on the relationships between sides of a right triangle. Figure A7 shows the relationship between the main trigonometric functions and the lengths of the sides x and y for the case when the length of the hypotenuse is equal to 1.

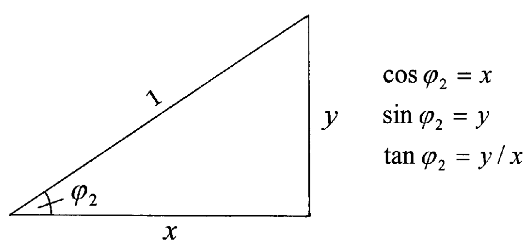

Figure A7. Three main conventional trigonometric functions.

The definitions of the conventional trigonometric functions are based on the transformations of the right triangle as a function of the non-right angle φ_2 shown in Figure A8. The main features of these transformations are:

- The triangles located at the two left quadrants are mirror images of the triangles located at the two right quadrants. Similarly, the triangles located at the two bottom quadrants are mirror images of the triangles located at the two top quadrants.

- When the length of the hypotenuse of the triangles is equal to 1, the ranges of the lengths of its sides x and y are between 0 and 1.

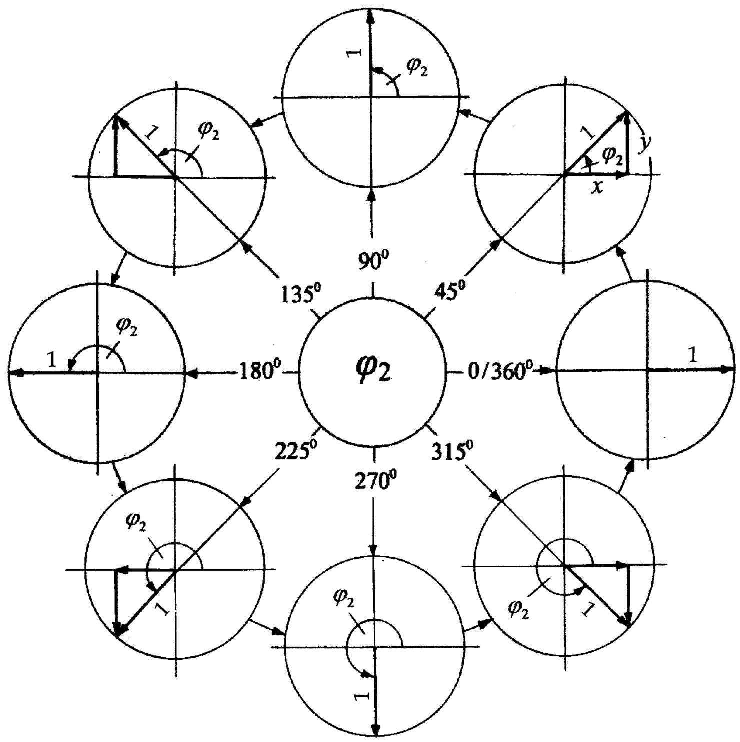

Figure A8. Appearances of a right triangle corresponding to the conventional trigonometry.

The 3D-SST uses the *toryx trigonometry* that employs the following relationship between the toryx trigonometric function $\cos t\varphi_2$ and the number b that extends from negative infinity $(-\infty)$ to positive infinity $(+\infty)$ as the angle φ_2 changes from 0 to 360^0:

$$\cos t\varphi_2 = x = \frac{b-1}{b+1} \qquad (0 < \varphi_2 < 360^0) \qquad \text{(A4-1)}$$

The letter t in the symbols of the toryx trigonometric functions differentiates the toryx trigonometric function from the conventional one. Figure A9 shows the transformations of the right triangle as a function of the angle φ_2 according to Eq. (A4-1). The main features of these transformations are (Table A2):

- When the angle φ_2 is between 0 and 180^0 the appearances of the right triangles in the toryx trigonometry are the same as in the conventional trigonometry. Thus, within this range of the angle φ_2 the conventional and toryx trigonometry are identical.

- When the angle φ_2 is between 180 and 360^0, the right triangle of the toryx trigonometry becomes *outverted*. Consequently, the length of its horizontal side x becomes greater than 1, while the length of the other side y is expressed with imaginary numbers.
- When the angle φ_2 approaches 270^0 from a smaller angle, the length of its horizontal side x approaches positive real infinity $(+\infty)$, while the length of the other side y approaches positive imaginary infinity $(+\infty i)$.
- When the angle φ_2 approaches 270^0 from a greater angle, the length of its horizontal side x approaches negative real infinity $(-\infty)$, while the length of the other side y approaches negative imaginary infinity $(-\infty i)$.
- When the angle φ_2 approaches 360^0 from a smaller angle, the length of its horizontal side x approaches 1, while the length of the other side y approaches tnegative imaginary infinility $(-0i)$.

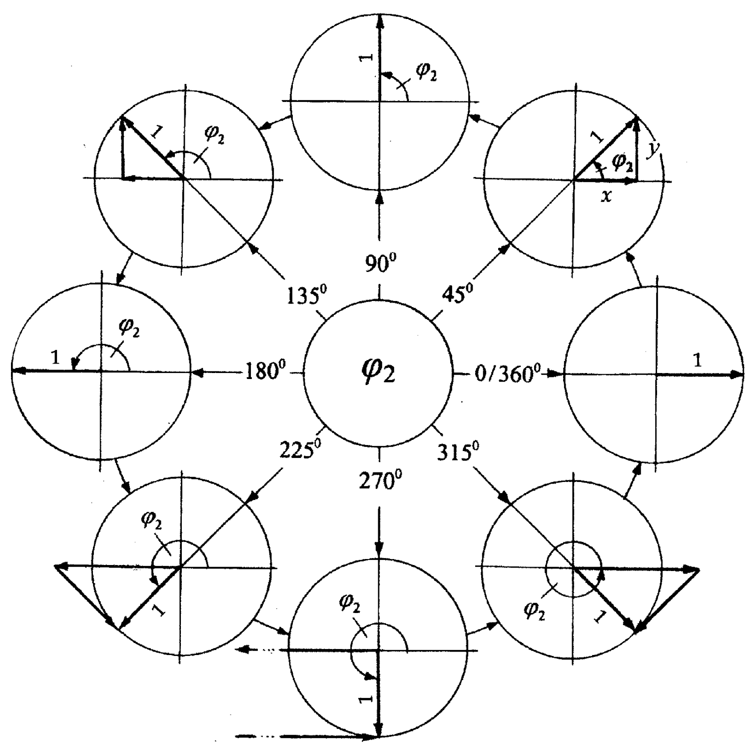

Figure A9. Appearances of a right triangle corresponding to the toryx trigonometry.

Table A2. Relationship between toryx and conventional trigonometric functions.

Toryx	Conventional	
$(0<\varphi_2<360^0)$	$(0<\varphi_2<180^0)$	$(180<\varphi_2<360^0)$
$\cos t(\varphi_2)$	$\cos(\varphi_2)$	$\sec(\varphi_2)$
$\sin t(\varphi_2)$	$\sin(\varphi_2)$	$i\tan(\varphi_2)$

5 Toryx number line vs conventional number line

Figure A10 shows a conventional number line as a set of real numbers b extended along a straight line from the zero to the right side towards positive infinity $(+\infty)$ and to the left side towards negative infinity $(-\infty)$.

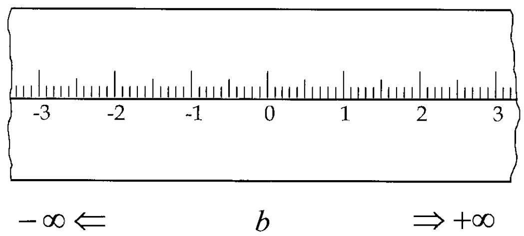

Figure A10. Conventional number line.

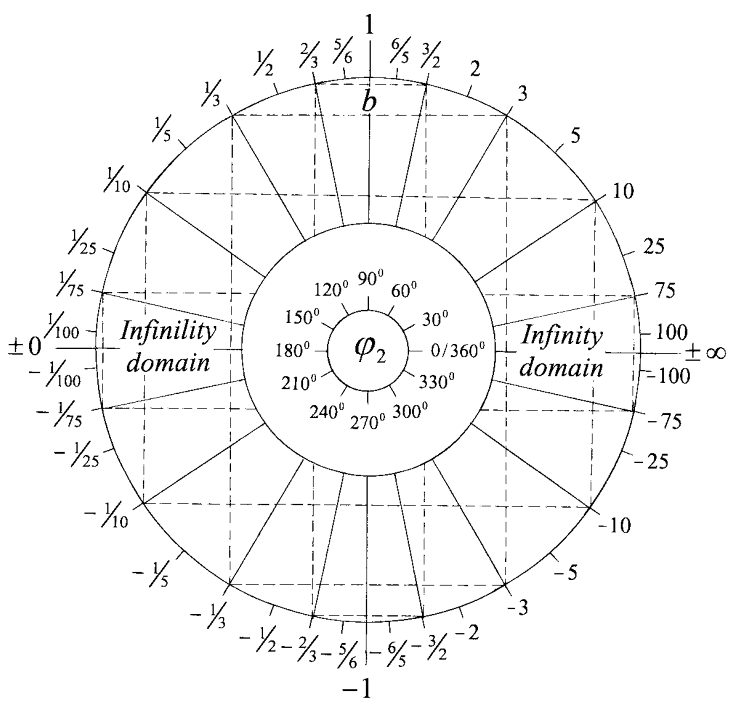

Figure A11. Toryx number line.

Unlike the conventional linear number line the toryx number line is circular. As shown in Figure A11, in the toryx number line, a set of real numbers b is extended counterclockwise along a circle from positive infinity $(+\infty)$ to negative infinity $(-\infty)$. The relationship between the numbers b and the polar angle φ_2 on the toryx number line is based on the toryx trigonometry. Thus, we obtain from Eq. (A4-1):

$$b = \frac{1+\cos t\varphi_2}{1-\cos t\varphi_2} \qquad (0^0 < \varphi_2 < 360^0) \qquad \text{(A5-1)}$$

Considering the relationship between conventional and toryx trigonometric functions shown in Table A2, we can present Eq. (A5-1) in terms of conventional trigonometry.

$$b = \frac{1+\cos\varphi_2}{1-\cos\varphi_2} \qquad (0^0 < \varphi_2 < 180^0) \qquad \text{(A5-2)}$$

$$b = -\frac{1+\cos\varphi_2}{1-\cos\varphi_2} \qquad (180^0 < \varphi_2 < 360^0) \qquad \text{(A5-3)}$$

The toryx number line is divided into two domains, the *infinity domain* and the *infinility domain* occupying equal spaces on the number line. The infinity domain contains the numbers b extending clockwise from the positive unity $(+1)$ to the negative unity (-1). It occupies both top and bottom right quadrants of the number line. Within the top right quadrant $(+0^0 < \varphi_2 < 90^0)$ the numbers b increase from the positive unity $(+1)$ to positive infinity $(+\infty)$, while within the bottom right quadrant $(270^0 < \varphi_2 < 360^0)$ the numbers b decrease from the negative unity (-1) to negative infinity $(-\infty)$.

The infinility domain contains the numbers b extending counterclockwise from the positive unity $(+1)$ to the negative unity (-1). It resides in two left quadrants of the number line. Within the top left quadrant $(90^0 < \varphi_2 < 180^0)$ the numbers b decrease from the positive unity $(+1)$ to positive infinility $(+0)$, while within the bottom left quadrant $(180^0 < \varphi_2 < 270^0)$ the numbers b decrease from negative infinility (-0) to the negative unity (-1). Notably, negative infinity $(-\infty)$ merges with positive infinity $(+\infty)$ when $\varphi_2 \to 0/360^0$, while positive infinility $(+0)$ merges with negative infinility (-0) when $\varphi_2 \to 180^0$.

There are two kinds of polarization between the numbers b of the toryx number line, inverse and reverse:

Inverse polarization - The magnitudes of the numbers b'' located in the left quadrants are inversed in respect to the magnitudes of the numbers b' located in the right quadrants. Thus,

$$b'' = \frac{1}{b'} \qquad \text{(A5-4)}$$

Reverse polarization - The numbers located in the top quadrants b' and the bottom quadrants b'' have same magnitudes but reversed signs. Thus,

$$b'' = -b' \qquad \text{(A5-5)}$$

6 Velocities of the toryx trailing string

Figure A12 shows transformations of a hodograph of velocities of trailing string at the middle point *a* of trailing string (Fig. A3) as its steepness angle φ_2 increases from 0 to 360^0. The hodograph forms a right triangle which sides represent the relative translational velocity β_{2t} and the relative rotational velocity β_{2r} of trailing string, while its hypotenuse represents the relative spiral velocity β_2 = 1 of this string. Notably, the hodograph of velocities of trailing string uses the toryx trigonometry.

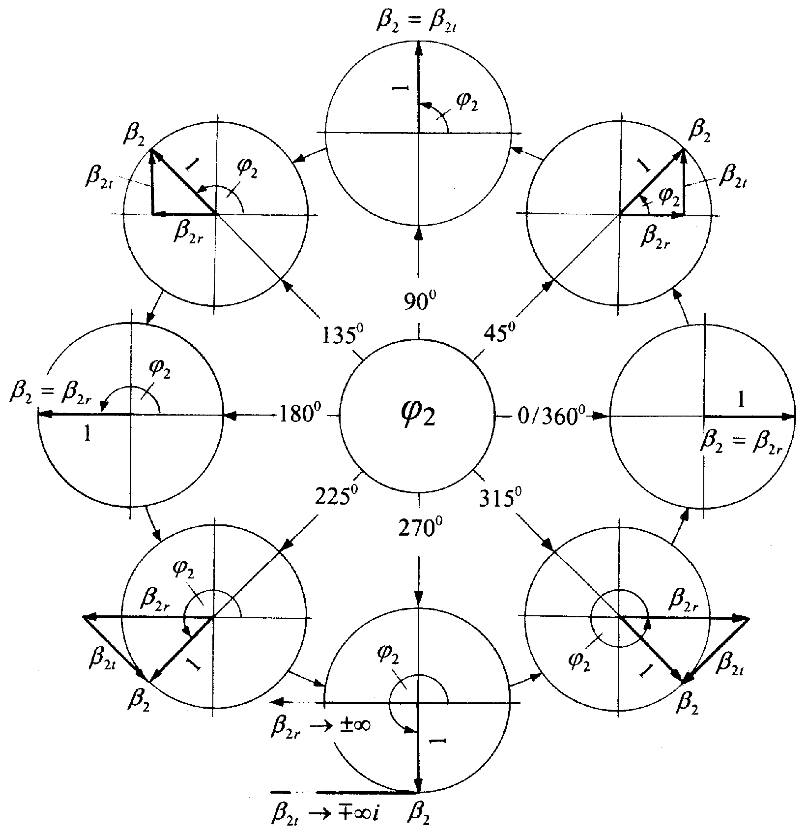

Figure A12. Transformations of a hodograph of velocities at middle point *a* (Fig. A3).

To maintain spacetime integrity of the toryx, as its trailing string propagates at a constant relative spiral velocity $\beta_2 = 1$, the relative translational and rotational velocities, β_{2t} and β_{2r}, must vary in a very specific way. As shown in Fig. A13 the translational velocity at each point of the trailing string must be proportional to the distance of said point from the toryx center. At the same time, the rotational velocity of the trailing string must vary to satisfy equation (A1-3), according to which the trailing string must propagate at a constant relative spiral string velocity $\beta_2 = 1$.

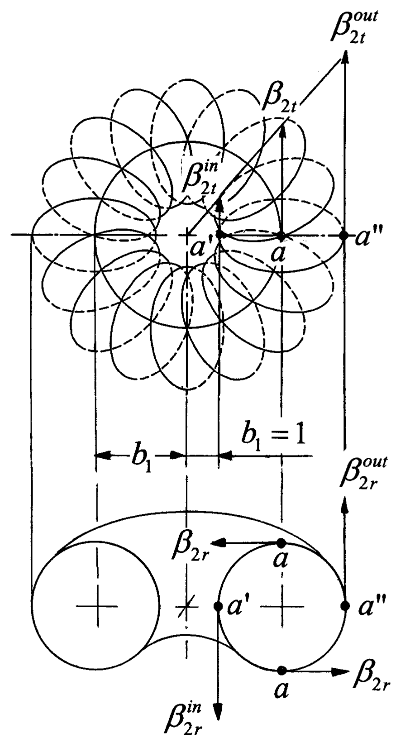

Figure A13. Relative peripheral velocities of the trailing string.

Table A3 shows equations for relative peripheral translational and rotational velocities of the trailing string. Within the ranges of b_1 (A6-5) and (A6-6) the inner and outer peripheral translational velocities β_{2t}^{in} and β_{2t}^{out} of the trailing string exceed the velocity of light.

Table A3. Relative peripheral velocities of the trailing string.

Velocities *at the point* a'	**Velocities** *at the point* a''
$\beta_{2t}^{in} = \dfrac{\sqrt{2b_1 - 1}}{b_1^2}$ (A6-1)	$\beta_{2t}^{out} = \dfrac{(2b_1 - 1)^{3/2}}{b_1^2}$ (A6-2)
$\beta_{2r}^{in} = \dfrac{\sqrt{b_1^4 - 2b_1 + 1}}{b_1^2}$ (A6-3)	$\beta_{2r}^{out} = \dfrac{\sqrt{b_1^4 - (2b_1 - 1)^3}}{b_1^2}$ (A6-4)
$0.544 < b_1 < 1.0$ (A6-5)	$1.0 < b_1 < 6.222$ (A6-6)

Figure A14 shows the variation of the relative instant translational and rotational velocities, β_{2t}^{i} and β_{2r}^{i}, for the case when $b_1 = 2$. Notably, between 0.25 and 0.75 portions of the cycle of the trailing string, β_{2t}^{i} exceeds the velocity of light while β_{2r}^{i} is expressed with imaginary numbers.

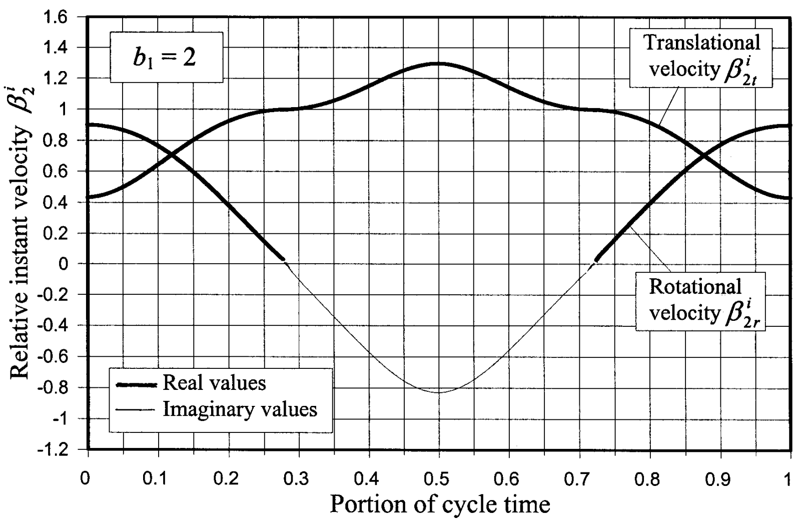

Figure A14. Variation of instant velocities β^i_{2t} and β^i_{2r} of the trailing string within one cycle of trailing string.

7 Classification of toryces

We use two integrated spacetime parameters of toryces to define their main classification: the *toryx vorticity* V and the *toryx reality* R. The toryx vorticity V is equal to the ratio of the radius of trailing string r_2 to the radius of leading string r_1 with the opposite sign.

$$V = -\frac{r_2}{r_1} = -\frac{b_2}{b_1} = -\frac{b_1 - 1}{b_1} = -\frac{b - 1}{b + 1} = -\cos t\varphi_2 \qquad \text{(A7-1)}$$

Figure A15 shows a circular diagram of the toryx vorticity V as a function of the steepness angle of trailing string φ_2. Toryces with positive vorticity V are called *positive* and with negative vorticity V, *negative.* This diagram can be treated as a proposed *toryx number line for the real numbers V*.

The circular diagram of the toryx vorticity V is divided into two domains, infinity domain and infinility domain, each occupying equal sectors of the diagram. The infinility domain occupies two top quadrants; it contains the values of V extending clockwise from the positive unity $(+1)$ and passing through infinility (± 0) to the negative unity (-1). The infinity domain resides in two bottom quadrants; it contains the values of V extending counterclockwise from the positive unity $(+1)$ and passing through infinity $(\pm\infty)$ to the negative unity (-1). Notably, positive infinility $(+0)$ merges with negative infinility (-0) at $\varphi_2 \to 90^0$, while negative infinity $(-\infty)$ merges with positive infinity $(+\infty)$ at $\varphi_2 \to 270^0$. There are two kinds of symmetrical polarization between the toryx vorticities V of the toryces that belong to the four quadrants of the circular diagram, inverse-symmetrical and reverse-symmetrical.

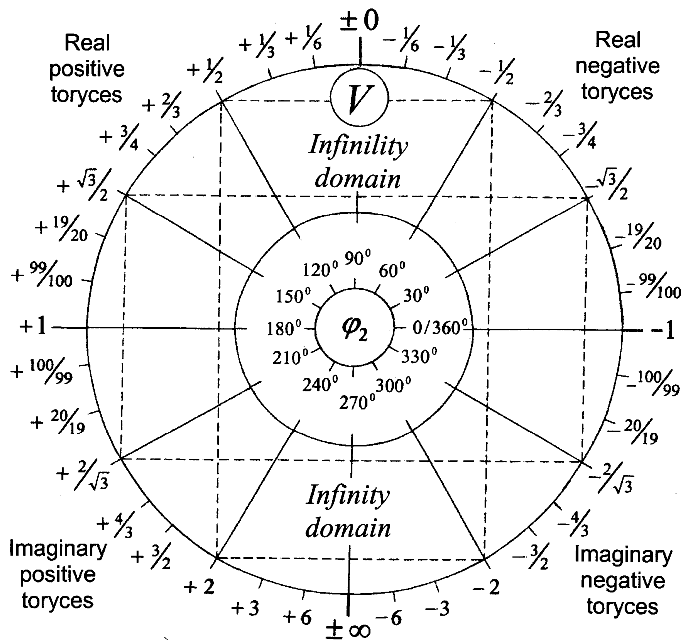

Figure A15. Toryx vorticity V as a function of the steepness angle of trailing string φ_2.

The toryces that belong to the top and bottom quadrants are inverse-symmetrically polarized by their vorticity V, because the magnitudes of their vorticities V are symmetrically inversed while the signs of V are the same. The toryces that belong to the right and left quadrants are reverse-symmetrically polarized by their vorticity V, because the signs of their vorticities V are symmetrically reversed while the magnitudes of V are the same.

The toryx reality R is equal to the toryx relative peripheral radius b.

$$R = b = 2b_1 - 1 = \frac{1+\cos t\varphi_2}{1-\cos t\varphi_2} \qquad \text{(A7-2)}$$

Figure A16 shows a circular diagram of the toryx reality R as a function of the steepness angle of trailing string φ_2. In real toryces the toryx reality R is positive, while in imaginary toryces the toryx reality R is negative. This diagram can be treated as a proposed *toryx number line for numbers R*. The circular diagram of the toryx reality R is divided into infinility and infinity domains occupying left and right quadrants respectively. There are two kinds of symmetrical polarization between the values of the toryx reality R of the toryces that belong to the four quadrants of the circular diagram, inverse-symmetrical and reverse-symmetrical.

The toryces that belong to the right and left quadrants are inverse-symmetrically polarized by their reality R, because the magnitudes of their realities R are symmetrically inversed while the signs of R are the same. The toryces that belong to the top and bottom quadrants are reverse-symmetrically polarized by their reality *R*, because the signs of their realities *R* are symmetrically reversed while the magnitudes of *R* are the same.

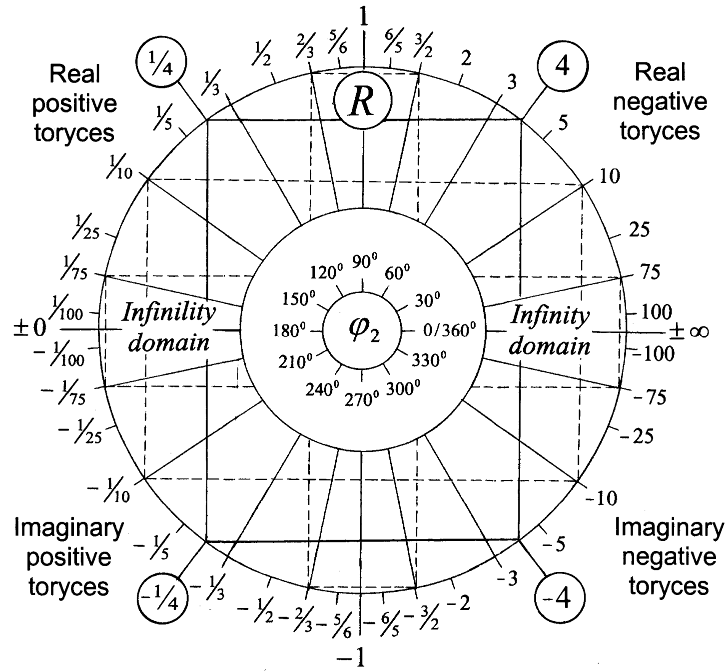

Figure A16. Toryx reality *R* as a function of the steepness angle of trailing string φ_2.

The toryces are divided into four main groups according to their vorticity *V* and reality *R*:

- Real negative toryces $(V < 0, R > 0)$, $(0^0 < \varphi_2 < 90^0)$
- Real positive toryces $(V > 0, R > 0)$, $(90^0 < \varphi_2 < 180^0)$
- Imaginary positive toryces $(V > 0, R < 0)$, $(180^0 < \varphi_2 < 270^0)$
- Imaginary negative toryces $(V < 0, R < 0)$, $(270^0 < \varphi_2 < 360^0)$.

8 Trends of spacetime parameters of toryces

Below are graphical presentations (Figs. A17 – A24) of trends of the toryx spacetime parameters as a function of the steepness angle of the trailing string φ_2 expressed by equations presented in Table A4. Also shown below each chart are main transformation points of toryces that occur at the borderlines between quadrants of circular diagrams of the toryx vorticity *V* (Fig. A15) and the toryx reality *R* (Fig. A16).

Table A4. Toryx relative spacetime parameters as a function of the steepness angle of trailing string φ_2 at the point *a* (Fig. A3).

Parameter	Leading string	Trailing string
Radius	$b_1 = \dfrac{1}{1-\cos t\varphi_2}$ (A8-1)	$b_2 = \dfrac{\cos t\varphi_2}{1-\cos t\varphi_2}$ (A8-2)
Wavelength	$\eta_1 = 1$ (A8-3)	$\eta_2 = \sqrt{\dfrac{1+\cos t\varphi_2}{1-\cos t\varphi_2}}$ (A8-4)
Length of one winding	$l_1 = \dfrac{1}{1-\cos t\varphi_2}$ (A8-5)	$l_2 = \dfrac{1}{1-\cos t\varphi_2}$ (A8-6)
The number of windings	$w_1 = 1$ (A8-7)	$w_2 = \dfrac{1}{\sin t\varphi_2}$ (A8-8)
Translational velocity	$\beta_{1t} = 0$ (A8-9)	$\beta_{2t} = \sin t\varphi_2$ (A8-10)
Rotational Velocity	$\beta_{1r} = \sin t\varphi_2$ (A8-11)	$\beta_{2r} = \cos t\varphi_2$ (A8-12)
Spiral velocity	$\beta_1 = \sin t\varphi_2$ (A8-13)	$\beta_2 = 1$ (A8-14)
Frequency	$\delta_1 = \sin t\varphi_2(1-\cos t\varphi_2)$ (A8-15)	$\delta_2 = 1-\cos t\varphi_2$ (A8-16)
Cycle time	$\tau_1 = \dfrac{1-\cos t\varphi_2}{\sin t\varphi_2}$ (A8-17)	$\tau_2 = \dfrac{1}{1-\cos t\varphi_2}$ (A8-18)

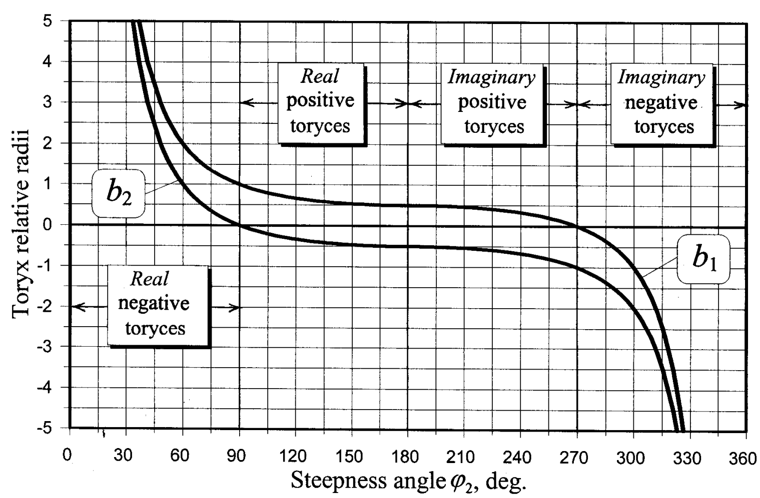

φ_2	$360/0^0$	90^0	180^0	270^0
b_1	$-\infty/+\infty$	$+1$	$+½$	$+0/-0$
b_2	$-\infty/+\infty$	$+0/-0$	$-½$	-1

Figure A17. Relative radii of leading and trailing strings, b_1 and b_2, as a function of the steepness angle of trailing string φ_2.

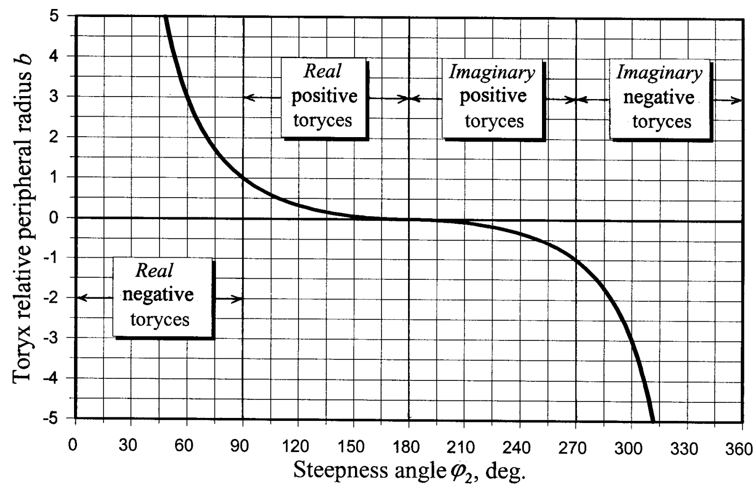

φ_2	$360/0^0$	90^0	180^0	270^0
b	$-\infty/+\infty$	$+1$	$+0/-0$	-1

Figure A18. Relative toryx outer radius b as a function of the steepness angle of trailing string φ_2.

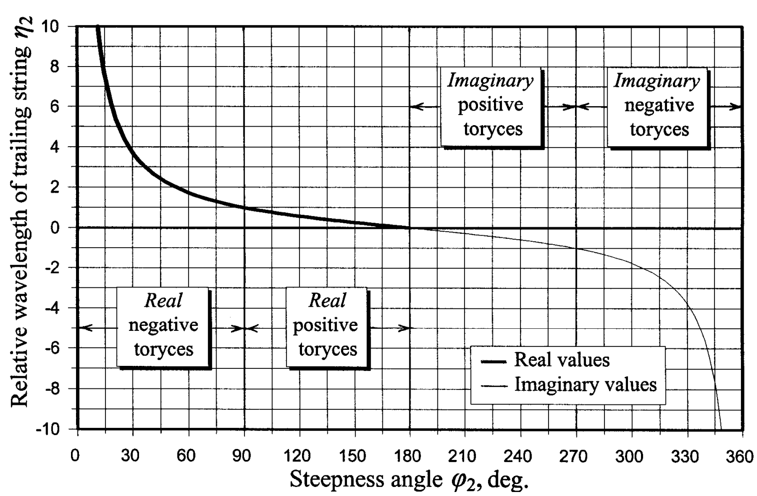

φ_2	$360/0^0$	90^0	180^0	270^0
η_2	$-\infty i/+\infty$	$+1$	$+0/-0i$	$-i$

Figure A19. Relative wavelength of the trailing strings η_2 as a function of the steepness angle of trailing string φ_2.

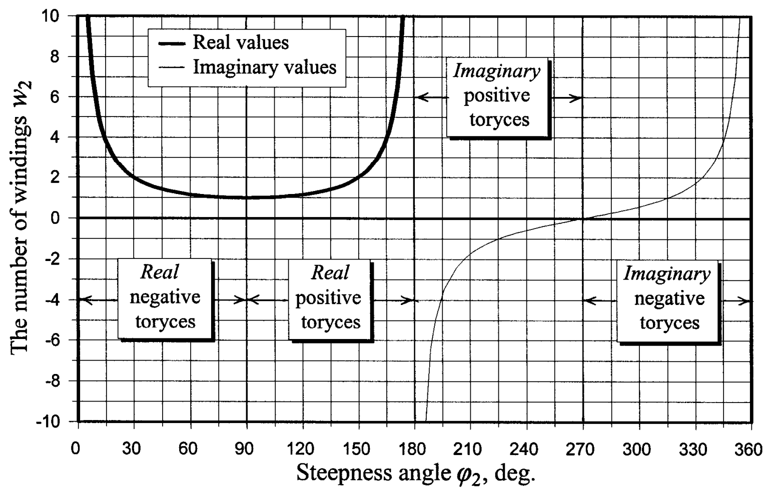

φ_2	$360/0^0$	90^0	180^0	270^0
w_2	$+\infty i/+\infty$	$+1$	$+\infty/-\infty i$	$-0i/+0i$

Figure A20. The number of windings of the trailing strings w_2 as a function of the steepness angle of trailing string φ_2.

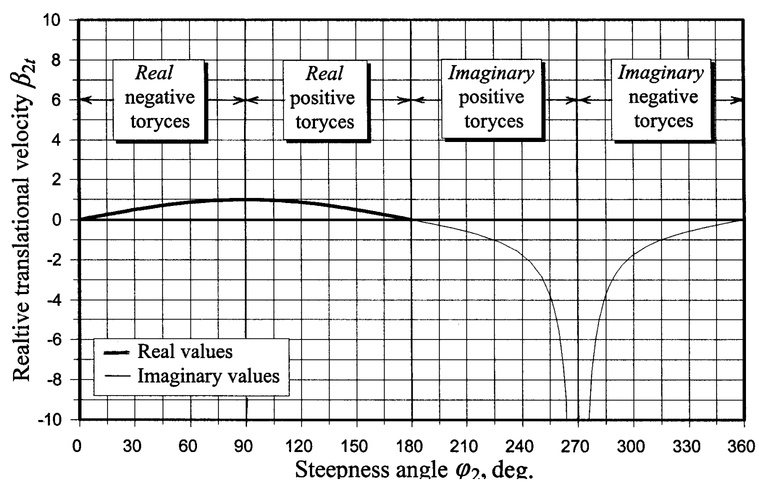

φ_2	$360/0^0$	90^0	180^0	270^0
β_{2t}	$-0i/+0$	$+1$	$+0/-0i$	$-\infty i$

Figure A21. Relative translational velocity of the trailing strings β_{2t} as a function of the steepness angle of trailing string φ_2.

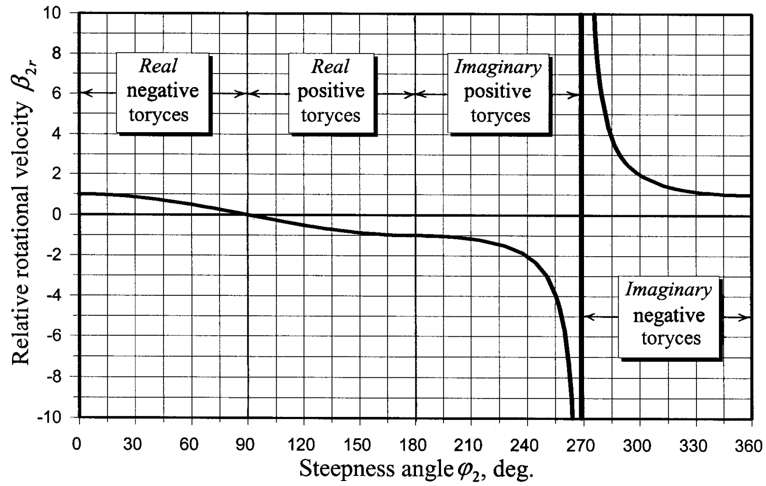

φ_2	$360/0^0$	90^0	180^0	270^0
β_{2r}	$+1$	$+0/-0$	-1	$-\infty/+\infty$

Figure A22. Relative rotational velocity of the trailing strings β_{2r} as a function of the steepness angle of trailing string φ_2.

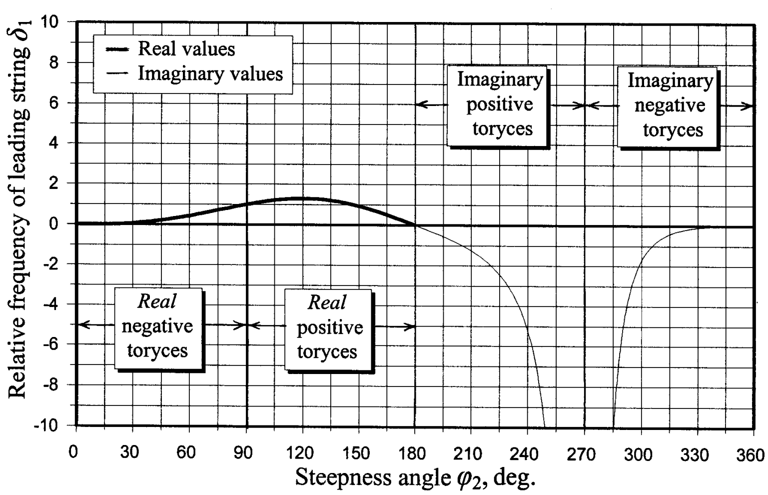

φ_2	$360/0^0$	90^0	180^0	270^0
δ_1	$-0i/+0$	$+1$	$+0/-0i$	$-\infty i$

Figure A23. Relative frequency of leading strings δ_1 as a function of the steepness angle of trailing string φ_2.

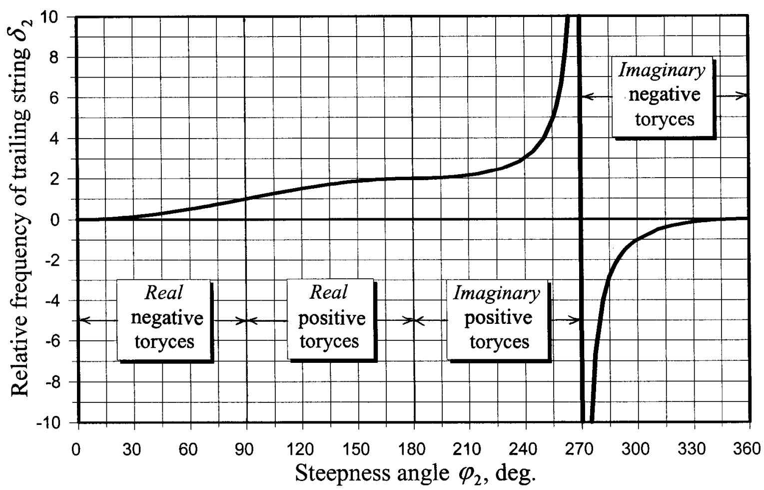

φ_2	$360/0^0$	90^0	180^0	270^0
δ_2	$-0/+0$	$+1$	$+2$	$+\infty/-\infty$

Figure A24. Relative frequency of trailing strings δ_2 as a function of the steepness angle of trailing string φ_2.

9 Toryx spacetime topology

Spacetime topology of the toryx includes inversions of its leading and trailing strings. To illustrate the inversion of its circular leading string let us envision it in the form of an extremely thin and narrow circular ribbon with the radius r_1 (Fig. A25). We assume that the leading string is propagating outward when $r_1 > 0$. In that case, the outer color of the ribbon is black, while its inner color is white.

As r_1 decreases while remaining positive, the ribbon begins to appear smaller, but still propagating outward. When the ribbon radius r_1 approaches positive infinility(+0), the ribbon reduces to the infipoint. After the ribbon radius becomes negative ($r_1 < 0$), the ribbon turns inside out, or becomes inverted, making its external color white and the internal color black.

To illustrate the inversion of the trailing string let us envision it in the form of an extremely thin and narrow toroidal ribbon (Fig. A26). We assume that the trailing string propagates outward when the radius of leading string r_1 is greater than the radius of real inversion string r_i ($r_1 > r_i$). In this case, the radius of the trailing string is positive ($r_2 > 0$) and the outer color of the toroidal ribbon is black, while its inner color is white. As r_1 decreases while remaining greater than r_i, the radius of the trailing string r_2 likewise decreases but remains positive. Consequently, the toroidal ribbon will appear slimmer and will have fewer windings w_2.

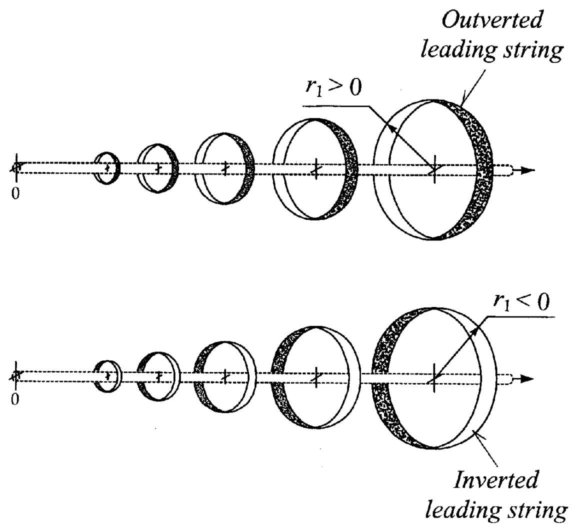

Fig. A25. Inversion of leading string.

When r_1 becomes infinitesimally close to the radius of real inversion string r_i, the radius of the trailing string r_2 approaches positive infinility (+0). So, the toryx reduces to a circle seen in Figure A26 as a colorless edge of a circular ribbon. When $r_1 < r_i$, the sign of the radius r_2 changes from positive to negative and the ribbon becomes inverted. Consequently, its outer color becomes white while its inner color becomes black.

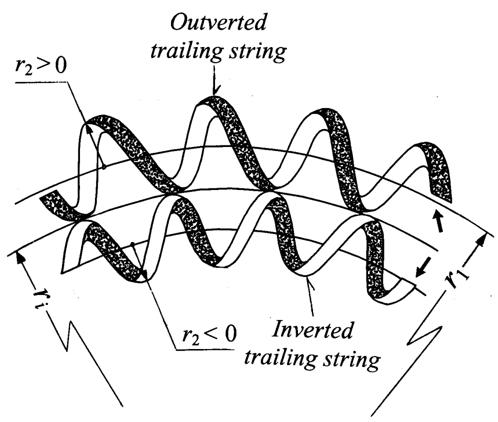

Fig. A26. Inversion of the trailing string.

Figure A27 shows metamorphoses of the toryx leading and trailing strings as a function of the steepness angle of trailing string φ_2. Four kinds of *inversion toryces* are located at the boundaries of the circular diagram between the four main groups of toryces.

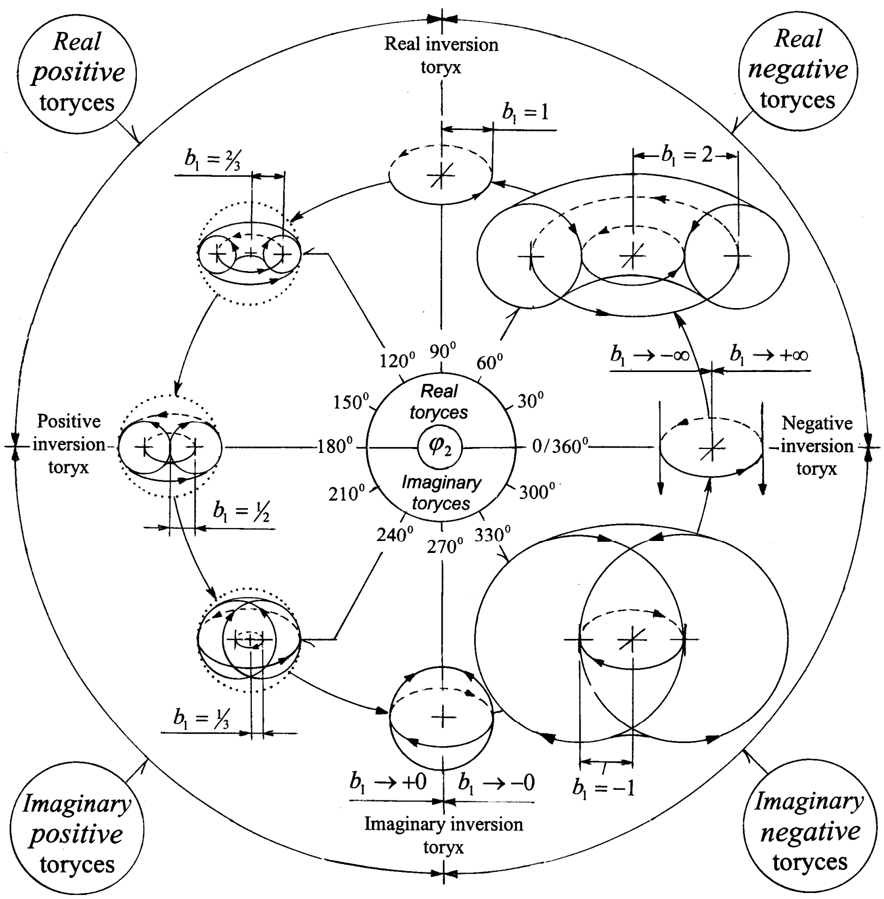

Figure A27. Metamorphoses of the toryx leading and trailing strings as a function of the steepness angle of the trailing string φ_2

Negative inversion toryx ($\varphi_2 \to +0^0/360^0$) - At this point, both leading and trailing strings become inverted. Thus, $b \to \pm\infty$ $b_1 \to \pm\infty$, $b_2 \to \pm\infty$. As φ_2 crosses the borderline at $0^0/360^0$ the toryx vorticity V remains negative, while the toryx reality R inverts from imaginary to real. The toryx appears as two parallel lines separated by the distance equal to the diameter real inversion string.

Real inversion toryx ($\varphi_2 \to 90^0$) – At this point, only trailing string becomes inverted. Thus, $b \to +1$ $b_1 \to +1$, $b_2 \to \pm 0$ and $w_2 \to +1$. As φ_2 crosses the borderline at 90^0, the toryx reality R remains real while its vorticity V inverts from negative to positive. It appears as circle with the relative radius $b_1 \to +1$.

Positive inversion toryx ($\varphi_2 \to 180^0$) – At this point, only spherical membrane becomes inverted. Thus, $b \to \pm 0$, $b_1 \to +1/2$, $b_2 \to -1/2$ and $w_2 \to +\infty/+\infty i$. As φ_2

crosses the borderline at 180⁰, the toryx vorticity V remains positive while its reality R inverts from real to imaginary. The toryx appears as an extreme case of a spindle torus with inner parts of its windings touching one another.

Imaginary inversion toryx ($\varphi_2 \to 270^0$) –At this point, only the leading string becomes inverted. Thus, $b \to -1$ $b_1 \to \pm 0$, $b_2 \to -1$ and $w_2 \to \pm 0$. As φ_2 crosses the borderline at 270^0, the toryx reality R remains imaginary while its vorticity V inverts from positive to negative. The toryx appears as a circle with the relative radius approaching -1. The circle is located at the plane perpendicular to the plane of the real inversion string

Located between the inversion toryces on the circular diagram of Figure A20 are the toryces that belong to their four main groups. Figures A28 and A29 show the transformations of toryces within each main group.

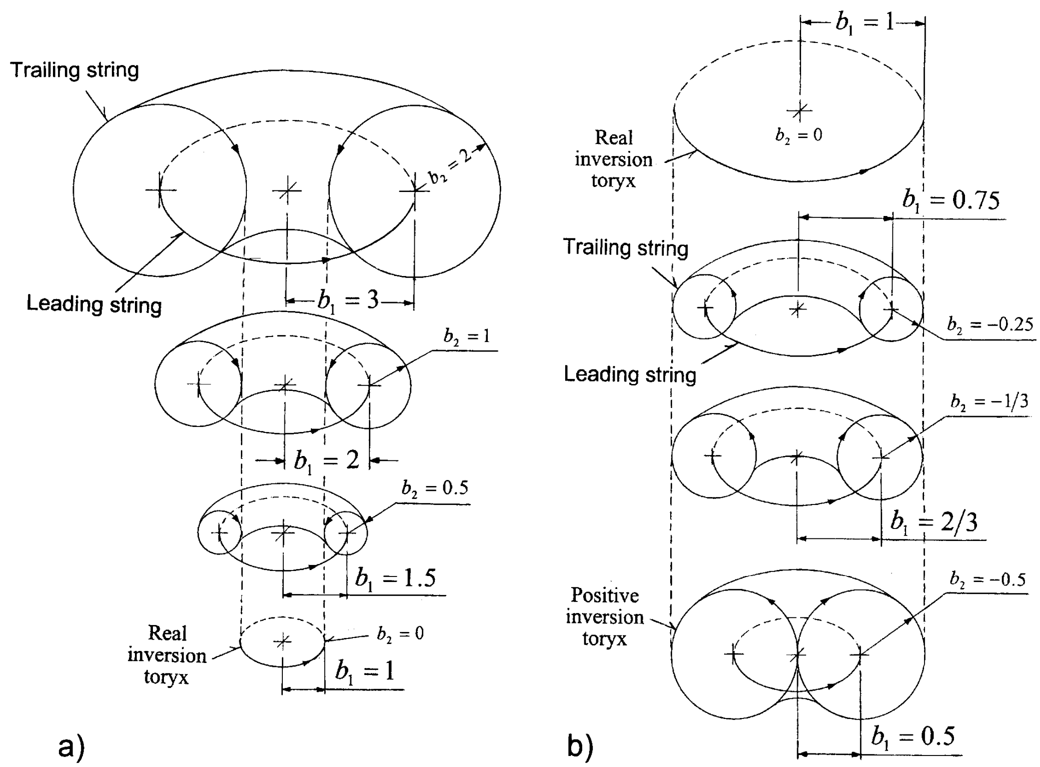

Figure A28. Metamorphoses of real toryces: a) negative and b) positive.

Real negative toryces (Fig. A28a) - These toryces belong to the top right quadrant of the circular diagram shown in Figure A27. Trailing strings of these toryces are wound counter-clockwise outside of the real inversion string. As φ_2 increases, b, b_1, b_2, and w_2 decrease, so that the trailing string appears like a conventional torus.

Real positive toryces (Fig. A28b) - These toryces belong to the top left quadrant of the circular diagram shown in Figure A27. Within this range the trailing string is inverted, so that its windings are now wound clockwise inside the real inversion toryx. As φ_2 increases, both b and b_1 decrease, but w_2 and negative values of b_2 increase. Consequently, the toryx appears as an inverted toroidal spiral.

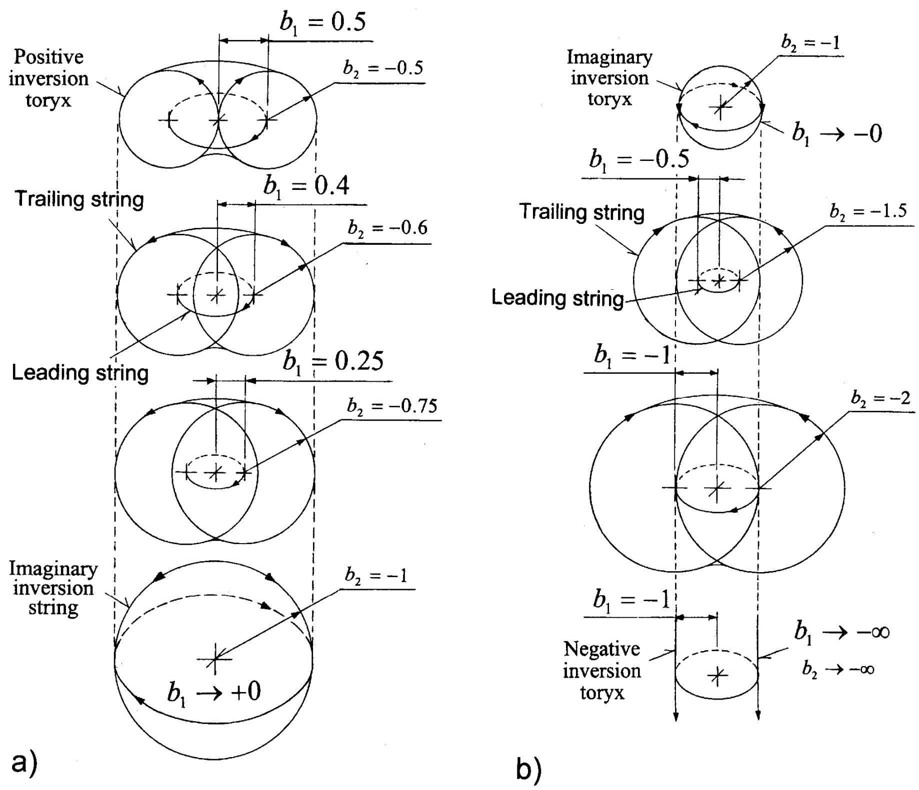

Figure A29. Metamorphoses of imaginary toryces: a) positive and b) negative.

Imaginary positive toryces (Fig. A29a) - These toryces belong to the bottom left quadrant of the circular diagram shown in Figure A27. Here b changes its sign from positive to negative and w_2 is expressed by negative imaginary numbers. As φ_2 increases, b_1 and negative imaginary values of w_2 decrease, while negative values of b and b_2 increase. Within this range, the trailing string is still inverted and its windings are wound inside the imaginary inversion toryx. The opposite parts of windings of the trailing string intersect with one another and the toryx appears as a spindle torus.

Imaginary negative toryces (Fig. A29b) - These toryces belong to the bottom right quadrant of the circular diagram shown in Figure A27. Here the leading string becomes inverted. As the negative value of b_1 increases, the negative values of b_2 also increase, while positive imaginary values of w_2 continue to increase too. Within this range trailing string propagates outward and its windings are located outside of the imaginary inversion toryx.

10 Toryx Law of Motion

According to the 3D-SST, toryces are created by the polarization of quantum vacuum. To maintain created toryces in polarized states, they must propagate in respect to one another according to the derived toryx law of motion. In application to the toryx this law is described by equation (A1-19) presenting the relative velocity of toryx leading β_1 as a function of the relative radius of toryx leading string as shown below:

$$\beta_1 = \frac{V_1}{c} = \frac{\sqrt{2b_1 - 1}}{b_1} \qquad \text{(A10-1)}$$

Notably, the toryx law of motion applied to toryces is more general than classical law of motion applicable to atomic electrons and celestial bodies for which $b_1 >> 1$. In these cases, equation (A10-1) reduces to the form:

$$\beta_1 = \sqrt{\frac{2}{b_1}} \qquad \text{(A10-2)}$$

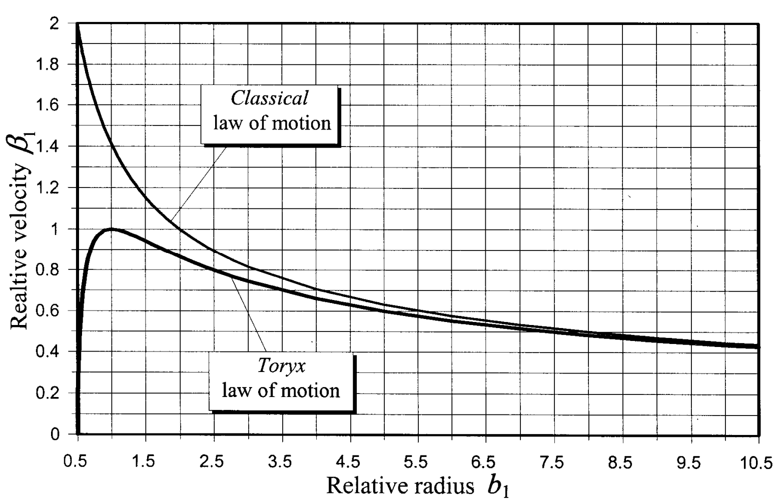

Figure 30. Toryx law of motion versus classical law of motion as a function of the relative radius of leading string b_1.

Figure A30 shows plots of equations (A10-1) and (A10-2). When $b_1 > 20$, the difference between the calculated values of β_1 from the toryx and classical laws of motion becomes very small; it continues to decrease as b_1 increases. But, as b_1 decreases from 20 to 2, this difference increases progressively. According to the classical law of motion, as b_1 decreases from 2 to 0, β_1 sharply increases and approaches positive infinity $(+\infty)$.

The toryx law of motion, however, yields a completely different trend of β_1 within the same range of b_1. Here, as b_1 decreases, β_1 initially increases and then, after reaching its maximum value of 1 (corresponding to the velocity of light c) at $b_1 = 1$, β_1 decreases sharply. Notably, in application to the atomic electron of the hydrogen atom at the ground level, the magnitude of b_1 is close to 40,000; for nucleons, however, magnitudes of $b_1 \leq 2$. This may explain why the classical law of motion cannot be applied to nucleons.

Acknowledgements

I am grateful to several scientists for making their valuable and stimulating comments on my ideas. Among them is Professor Carlo Rovelli (originally from Department of Physics and Astronomy of the University of Pittsburgh), who made encouraging comments on my idea of a multiple-level Universe. Thanks to the recommendations made by Dr. Akhlesh Lakhtakia (Department of Engineering and Mechanics, the Pennsylvania State University) I was able to publish the first three papers describing my initial ideas on this subject [9]-[11]. I appreciate my continuous communication with Mr. Nobuyuki Kanai from Osaka, Japan who followed my research on spirals for the last several years. I am very grateful to my daughter Ellen for stimulating my ideas regarding to the fine toryx structure and to my son Gene, whose spontaneous comments on the sizes of multiple universes had triggered my research on spirals almost two decades ago. He then created computer graphics for the covers of my books and provided a valuable technical support for publications and presentations of this subject.

References

[1] Bostick, W. Mass, Charge, and Current: The Essence of Morphology. *Physics Essays*, Vol. 4, No. 1, March 1991, pp. 45-59.

[2] J-L. Cambier and D.A. Micheletti, "Theoretical Analysis of the Electron Spiral Toroidal Concept," NASA/CR-2000-210654, Dec. 2000.

[3] Chen, C., Pakter, R. and Seward, D.C. Equilibrium and stability properties of self-organized electron spiral toroids. *Physics of Plasmas* Vol 8 (10), October 2001, pp. 4441-4449.

[4] Sarg, S. A Physical Model of the Electron According to the Basic Structure of Matter Hypothesis. *Physics Essays*, Vol. 16, No.2, 180-195, 2003.

[5] Penrose, R., *The Road to Reality - A Complete Guide to the Laws of the Universe*, Alfred A. Knopf, New York, 2005, pp. 965-91.

[6] C.W. Lucas, Jr. A Classical Electromagnetic Theory of Elementary Particles Part 2, Interwining Charge-Fibers. *The Journal of Common Sense Science, Foundation of Science*, Vol. 8 No. 2, May 2005.

[7] Gauthier, R.F. FTL Quantum Models of the Photon and the Electron," *AIP Conf. Proc.* Vol. 880, January 30, 2007, pp. 1099-1108.

[8] Gauthier, R.F. FTL Quantum Models of the Photon and the Electron. http://superluminalquantum.org/STAIF-2007paper.pdf.

[9] Ginzburg, V.B., "Toroidal Spiral Field Theory," *Speculations in Science and Technology*, Vol. 19, 1996.

[10] Ginzburg, V.B., "Structure of Atoms and Fields," *Speculations in Science and Technology*, Vol. 20, 1997.

[11] Ginzburg, V.B., "Double Helical and Double Toroidal Spiral Fields," *Speculations in Science and Technology*, Vol. 22, 1998.

[12] Ginzburg, V.B., *The Unification of Strong, Gravitational & Electric Forces,* Helicola Press, IRMC, Inc., 2003.

[13] Ginzburg, V.B., "The Relativistic Torus and Helix as the Prime Elements of Nature," *Proceedings of the Natural Philosophy Alliance*, Vol. 1, No. 1, Spring 2004.

[14] Ginzburg, V.B., *Prime Elements of Ordinary Matter, Dark Matter & Dark Energy*, Helicola Press, IRMC, Inc., 2006.

[15] Ginzburg, V.B., *Prime Elements of Ordinary Matter, Dark Matter & Dark Energy* – Beyond Standard Model & String Theory, The second revised edition, Universal Publishers, Boca Raton, Florida, 2007.

[16] Ginzburg, V.B., *Prime Elements of Ordinary Matter, Dark Matter & Dark Energy – Beyond Standard Model & String Theory*, The second revised edition, hard cover, www.lulu.com, 2007.

[17] Ginzburg, V.B., "The Origin of the Universe, Part 1: Toryces," *Proceedings of the Natural Philosophy Alliance, 17th Annual Conference of the NPA,* at California State University Long Beach, Vol. 7, 23-26 June 2010, pp. 162-78.

[18] Ginzburg, V.B., "Basic Concept of 3-Dimensional Spiral String Theory (3D-SST), "*Proceedings of the Natural Philosophy Alliance, 18th Annual Conference of the NPA,* at the University of Maryland, College Park, USA, Vol. 8, 6-9 July 2011, pp. 209-20.

[19] Seife, C., *Zero*, Viking, Published by the Penguin Group, Penguin Putnam, Inc. New York, USA, 2000.

[20] Lewis, H., *Geometry – A Contemporary Course*, Third Edition, McCormick-Mathers Publishing Company, Cincinnati, Ohio, 1973, pp. 6-8.